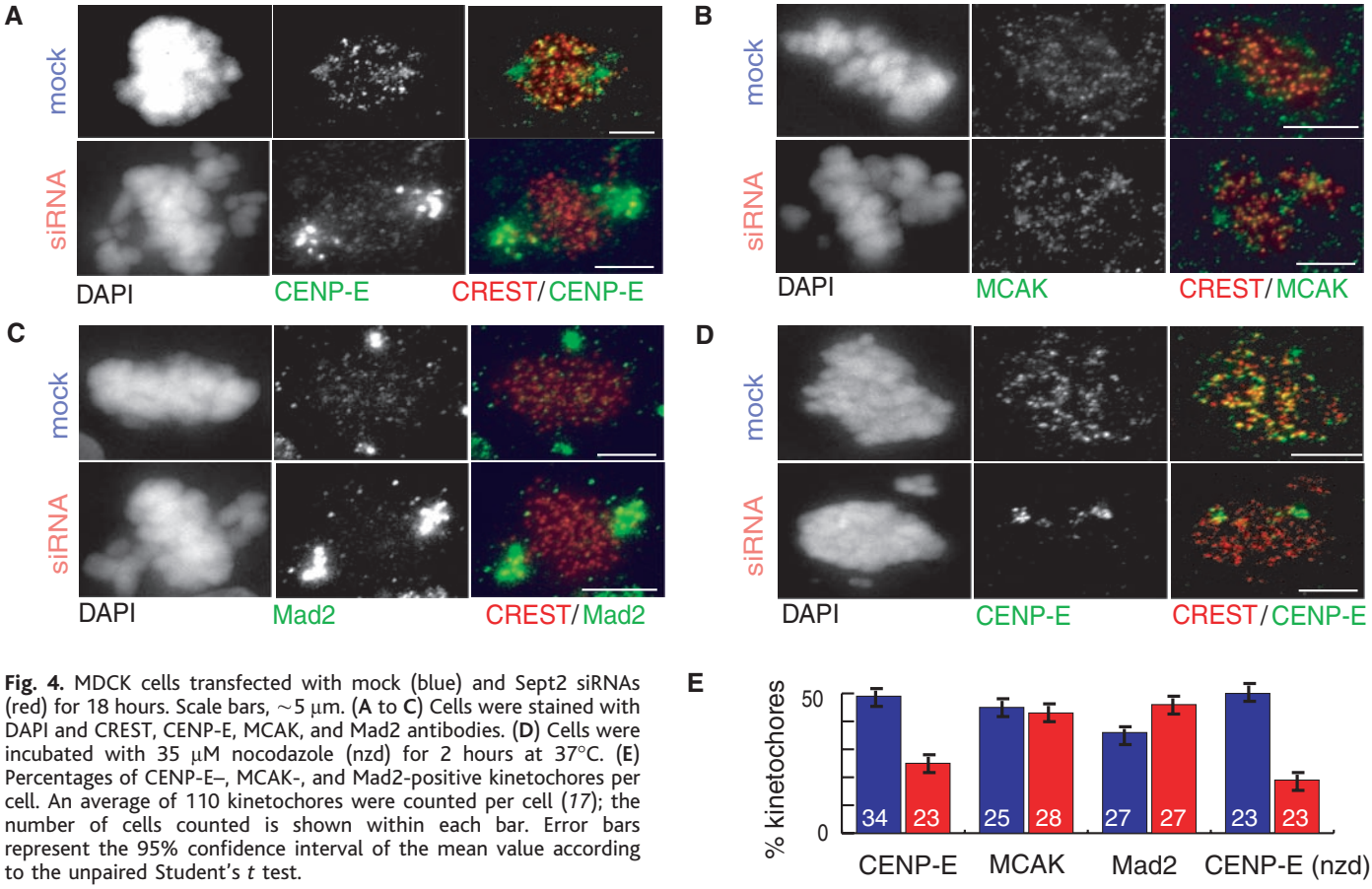

Fig. 4. MDCK cells transfected with mock (blue) and Sept2 siRNAs (red) for 18 hours. Scale bars, ~5 μm. (**A** to **C**) Cells were stained with DAPI and CREST, CENP-E, MCAK, and Mad2 antibodies. (**D**) Cells were incubated with 35 μM nocodazole (nzd) for 2 hours at 37°C. (**E**) Percentages of CENP-E–, MCAK-, and Mad2-positive kinetochores per cell. An average of 110 kinetochores were counted per cell (*17*); the number of cells counted is shown within each bar. Error bars represent the 95% confidence interval of the mean value according to the unpaired Student's *t* test.

Wong, and T. Yen for helpful advice and reagents. Supported by NIH grant GM35527 (W.J.N.) and by a research grant PRESTO from Japan Science and Technology Agency (M.K.). E.S. is a Jane Coffin Childs Memorial Fund postdoctoral fellow.

Supporting Online Material
www.sciencemag.org/cgi/content/full/307/5716/1781/DC1
Materials and Methods
Figs. S1 to S7
References
Movies S1 to S6

27 October 2004; accepted 26 January 2005
10.1126/science.1106823

Extrusion and Death of DPP/BMP-Compromised Epithelial Cells in the Developing *Drosophila* Wing

Matthew C. Gibson and Norbert Perrimon*

During animal development, epithelial cell fates are specified according to spatial position by extracellular signaling pathways. Among these, the transforming growth factor β/bone morphogenetic protein (TGF-β/BMP) pathways are evolutionarily conserved and play crucial roles in the development and homeostasis of a wide range of multicellular tissues. Here we show that in the developing *Drosophila* wing imaginal epithelium, cell clones deprived of the BMP-like ligand Decapentaplegic (DPP) do not die as previously thought but rather extrude from the cell layer as viable cysts exhibiting marked abnormalities in cell shape and cytoskeletal organization. We propose that in addition to assigning cell fates, a crucial developmental function of DPP/BMP signaling is the position-specific control of epithelial architecture.

The *Drosophila* wing primordium (imaginal disc) is a cellular monolayer that has invaginated and flattened to form a two-sided epithelial sac. During larval development, one side of this sac forms a thin squamous sheet, whereas the apposed epithelial surface adopts a pseudostratified columnar morphology (*1*, *2*). Although such range in epithelial form is common among metazoans and central to the morphogenesis of complex organ and appendage structures, very little is known about the molecular mechanisms that drive epithelia into their distinctive squamous, cuboidal, and columnar morphologies. To address this issue, we initiated a genetic screen for factors that control epithelial cell shape during *Drosophila* imaginal disc development.

To circumvent the embryonic lethality associated with many mutant alleles, we used the directed mosaic FLP/FRT system (*3*) to screen somatic cell clones homozygous for a collection of ethylmethane sulfonate (EMS)–induced lethal mutations. This approach uses a tissue-specific Gal4 driver (*T155-Gal4*) to direct expression of the *flipase* (*flp*) enzyme in developing epithelia, thus catalyzing a low frequency of mitotic recombination between an EMS-mutagenized FRT chromatid and its green fluorescent protein (GFP)–marked homolog. Within the disc epithelium, mitotic re-

Department of Genetics and Howard Hughes Medical Institute, Harvard Medical School, Boston, MA 02115, USA.

*To whom correspondence should be addressed. E-mail: perrimon@receptor.med.harvard.edu

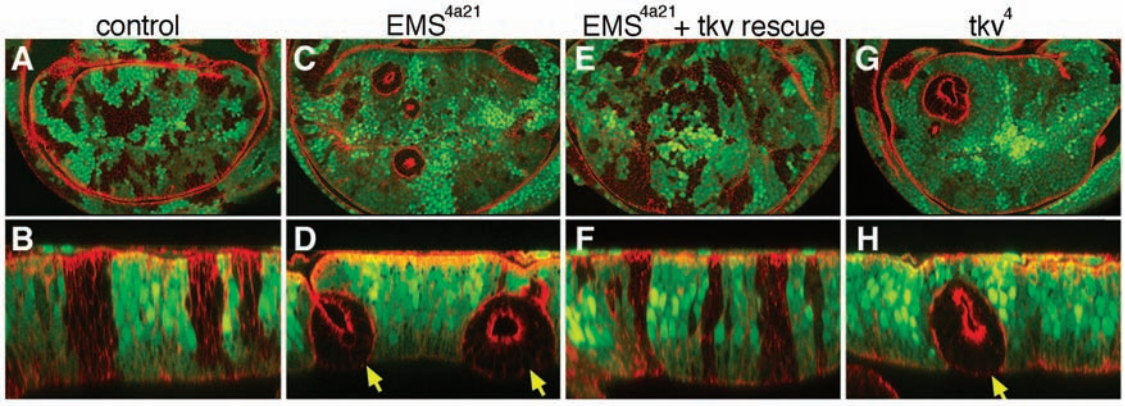

Fig. 1. Extrusion of *tkv* mutant clones from the wing disc. Clones lacking GFP (green) were stained for F-actin (ACT, red) to delineate cell outlines. Upper panels are standard confocal XY sections; the lower panels are XZ optical cross sections. Individual channel images of ACT and GFP are available in fig. S1. (**A** and **B**) Control clones lacking GFP expression. Note that GFP-negative cells integrate normally into the epithelial layer. (**C**) *EMS*^{4a21} mutant clones change shape and segregate from control cells, disrupting the continuity of the epithelial layer. Also note the reduced number of GFP-negative clones [compare (C) with (A)], indicative of intermittent clone cell death. (**D**) In XZ sections, *EMS*^{4a21} homozygous clones extrude basally as inverted epithelial cysts (yellow arrows). (**E** and **F**) Confirming *EMS*^{4a21} as an allele of *tkv*, *EMS*^{4a21} clone lethality and extrusion are rescued by expression of *UAS-tkv*. (**G** and **H**) *T155>flp*-induced *tkv*^{4} clones also extrude from the wing epithelium (yellow arrow), indicating that this phenotype is not allele specific.

combination events produce a GFP-negative cell clone homozygous for the mutation of interest as well as a corresponding "twin spot" identifiable by the presence of two copies of GFP. In this study, GFP-negative clones homozygous for a random series of EMS mutations were induced with *T155*-Gal4>UAS-*flp* (*T155>flp*) and stained with rhodamine-phalloidin to outline cell boundaries. Late third-instar wing imaginal discs were subsequently analyzed for clonal defects in epithelial morphogenesis (Fig. 1, A and B).

In the experimental line *EMS*^{4a21}, mutant clones in medial regions of the wing disc exhibited defects in the ability to establish or maintain the pseudostratified columnar cell shape, resulting in their retraction from the apical epithelial surface and subsequent basal extrusion (Fig. 1, C and D). Counts of clone frequency relative to twin spot controls indicated that many clones induced in the presumptive medial blade territory were not recovered, presumably as a result of cell death, but those that we did observe consistently presented as cystlike epithelial extrusions. In addition, a large number of extruding clones were observed in the presumptive hinge and notum regions of experimental discs, with a fraction of these protruding apically rather than extruding basally (*4*). We conclude that loss of the *EMS*^{4a21} gene product caused defective morphogenesis and clone extrusion, a phenotype intermittently associated with cell death in the medial wing blade territory.

To determine the genetic defect underlying extrusion, we mapped the embryonic lethality of *EMS*^{4a21} to cytological interval 25D-25F, which includes the transforming growth factor β (TGF-β) type I receptor *thickveins* (*tkv*) (*5*). As a transmembrane receptor for DPP/BMP ligand, TKV is crucial for imaginal disc development (*6*–*13*) and other developmental processes such as adult thorax closure and embryonic dorsal closure (*14*, *15*). Consistent with *EMS*^{4a21} representing an allele of *tkv*, *EMS*^{4a21} homozygotes exhibited embryonic

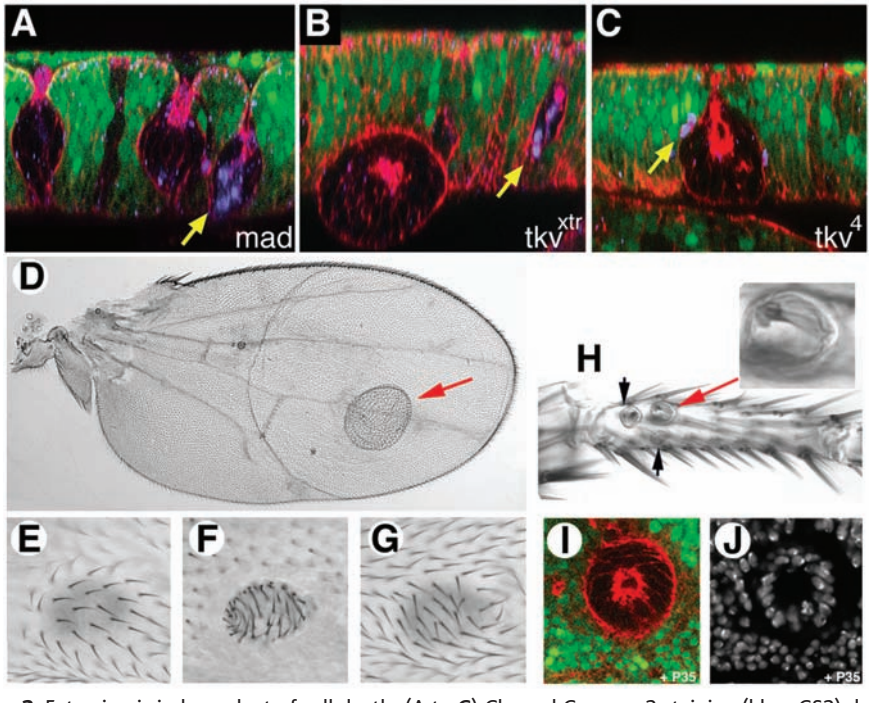

Fig. 2. Extrusion is independent of cell death. (**A** to **C**) Cleaved Caspase-3 staining (blue; CS3) does not correlate with (A) *mad*^{12}, (B) *tkv*^{xtr}, and (C) *tkv*^{4} clones marked by loss of GFP (green) and stained with phalloidin (red; ACT). Although some CS3-positive cells are indeed present (yellow arrows), many extruding clones show no evidence of cell death. (**D**) Adult wing containing a large *tkv*^{xtr} clone (red arrow). (**E** to **G**) Extruded cuticular vesicle (F) lodged between the dorsal (E) and ventral (G) wing surfaces. (**H**) *tkv*^{xtr} extrusions in the adult leg (arrows). The vesicle indicated by a red arrow contains a sensory bristle (inset), consistent with a high level of cellular functioning in extruded clones. (**I**) Extrusion of clones from the wing disc is not rescued by blocking apoptosis with *T155-Gal4>UAS-p35*. (**J**) DNA stain (DAPI; 4′,6′-diamidino-2-phenylindole) confirms normal nuclear morphology within the extruded clone shown in (I).

lethal phenotypes reminiscent of known *tkv* mutations (*16*), and *EMS*^{4a21} failed to complement the previously identified alleles *tkv*^{7} (n = 413), *tkv*^{4} (n = 386), and *tkv*^{K16159}(n = 319) (*5*). Confirming *EMS*^{4a21} as a *tkv* allele, a *UAS-tkv* construct expressed globally under *tubulin-Gal4* rescued *EMS*^{4a21}homozygotes to adult eclosion (*4*). More importantly, expression of *UAS-tkv* under *T155-Gal4* fully rescued *EMS*^{4a21} clone extrusion (Fig. 1, E and F), as did clone-autonomous expression of UAS-*tkv* using the MARCM system (fig. S2). These experiments demonstrate that clone extrusion was caused by loss of *tkv*, and we have therefore designated *EMS*^{4a21} as *tkv*^{extruded} (*tkv*^{xtr}).

We next used *T155Gal4>flp* to induce clones of the amorphic allele *tkv*^{4} (*5*) as well as an allele of the downstream signal transducer encoded by *mothers against DPP* (*mad*^{12})

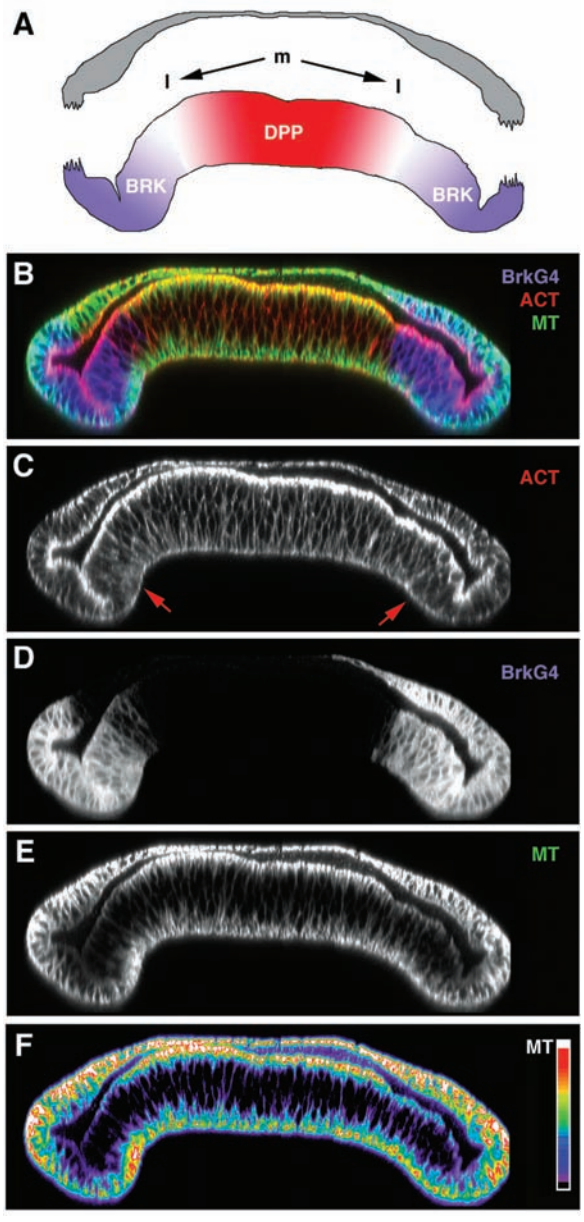

Fig. 3. A gradient of epithelial architecture spans the wing disc. (**A**) DPP represses *brk* throughout medial (m) wing disc cells. (**B** to **E**) *brk-Gal4>UAS-srcEGFP* (blue) disc stained for F-actin (ACT, red) and microtubules (MT, green). (**B**) The overlap between apical MTs and ACT appears as an apical yellow band that terminates in *brk*+ cells owing to the absence of apical microtubules. (**C**) Apical ACT is consistent along the medial-to-lateral axis, but ACT association with the basolateral cortex weakens laterally (red arrows). (**D**) *brk-Gal4>srcEGFP* demarcates the lateral domains where DPP signaling is low. (**E**) Apical microtubule densities are robust in medial columnar cells where DPP/BMP signal is high but weaken in lateral *brk* domains. (**F**) Pixel intensity plot of (E) illustrates an apical-specific gradient in microtubule intensity, because basal MT staining is consistent along the medial-lateral axis.

(*5*). In both cases, extrusion was routinely observed (Fig. 1, G and H, and Fig. 2A), linking this phenotype to general defects in DPP/BMP signaling and not some unique effect of the tkv^{xtr} allele. These results contrast with the current interpretation of DPP/BMP as a cell survival factor, which is based on the observation that *tkv* mutant cells are eliminated from the wing by proapoptotic c-Jun N-terminal kinase (JNK) signaling (*17*–*20*). We thus considered whether extrusion might reflect a preliminary stage of apoptosis, similar to the basal extrusion of vertebrate epithelial cells destined for death (*21*). However, four observations provide evidence against this idea. (i) Clonal loss of mad^{12}, tkv^{xtr}, or tkv^{4} consistently caused extrusion, but this phenotype did not necessarily correlate with apoptosis indicated by Caspase-3 activation (Fig. 2, A to C). (ii) Extruded tkv^{xtr} and tkv^{4} clones often grew to an appreciable size (Fig. 1, D and H, and Fig. 2B) and contained mitotic figures (fig. S3), which is inconsistent with their active engagement in an apoptotic pathway. (iii) Many extruded clones survived metamorphosis and differentiated inverted cuticular vesicles lodged between the dorsal and ventral surfaces of the adult wing or leg (Fig. 2, D to H), demonstrating that *tkv* loss can disrupt epithelial organization without compromising cell viability. (iv) Extrusion was unaffected by ectopic expression of the apoptosis inhibitor p35 (Fig. 2, I and J), confirming that this phenotype is not simply a secondary consequence of cell death.

Together, these results challenge the view of DPP/BMP as a survival factor, favoring instead a more direct role for this pathway in controlling epithelial morphogenesis. This interpretation has the advantage of unifying the role of DPP/BMP as a pattern morphogen in imaginal discs with its role as an agent of morphogenesis in other developmental contexts. Nevertheless, the large phenotypic discrepancy between clone extrusion and clone death necessitated a closer consideration of why our results differed from previous reports. A major procedural difference in our experiments was the use of *T155>flp* to induce clones, instead of heat shock (*hs>flp*). Indeed, we confirmed that almost all heat shock–induced tkv^{4} and tkv^{xtr} clones were eliminated from the developing wing blade, as previously reported (*4*, *12*). This indicates that either the *hs>flp* method enhanced *tkv* clone death, or alternatively, the *T155>flp* method somehow enhanced clone viability. Both of these possibilities could be explained by differential background activity of the JNK stress signaling pathway, because decreasing JNK activity is sufficient to rescue the lethality of some *hs>flp*-induced *tkv* clones (*19*). Conversely, when we used a single mutant allele of the regulatory phosphatase *puckered* to increase background JNK activity (*18*), *T155>flp*-induced tkv^{xtr} clones were completely eliminated from the wing blade territory and extruding clones larger than 10 cells were not observed (fig. S4) (n = 15 discs). This contrasts sharply with normal circumstances, where 78% of discs had one large tkv^{xtr} extrusion greater than 10 cells in the wing blade and 50% had 2 or more (n = 32 discs).

Based on the observations above, we infer that the primary phenotype of *tkv* clones is extrusion and propose that JNK-dependent cell death is a potent and confounding secondary effect, similar to a wound response. Current models suggest that *tkv* clone-dependent JNK activation is triggered by a morphogen-sensing mechanism designed to correct discontinuities in the total DPP/BMP gradient (*19*, *22*). Our results suggest an alternative possibility: that the disruptive force of extrusion itself causes sufficient mechanical stress to activate JNK within and around *tkv* mutant cells (fig. S2C). Mechanical stretch, for example, activates JNK signaling in vertebrate cells (*23*), and mechanical disruption of the larval or adult epidermis causes localized JNK activation in *Drosophila* (*24*, *25*). Extending these observations to the wing disc, we used a finely sharpened tungsten needle to stretch, then pierce the imaginal epithelium, mimicking the effect of extrusion. This manipulation elicited localized JNK reporter activity similar to that seen in wounded larval and adult epidermis (*24*, *25*) and identical to that seen around *tkv* mutant clones (fig. S4).

Having concluded that the primary defect in *tkv* clones is extrusion and not death, we turned our attention to identifying position-specific aspects of epithelial morphogenesis that could be controlled by DPP/BMP signaling. During normal development, secreted

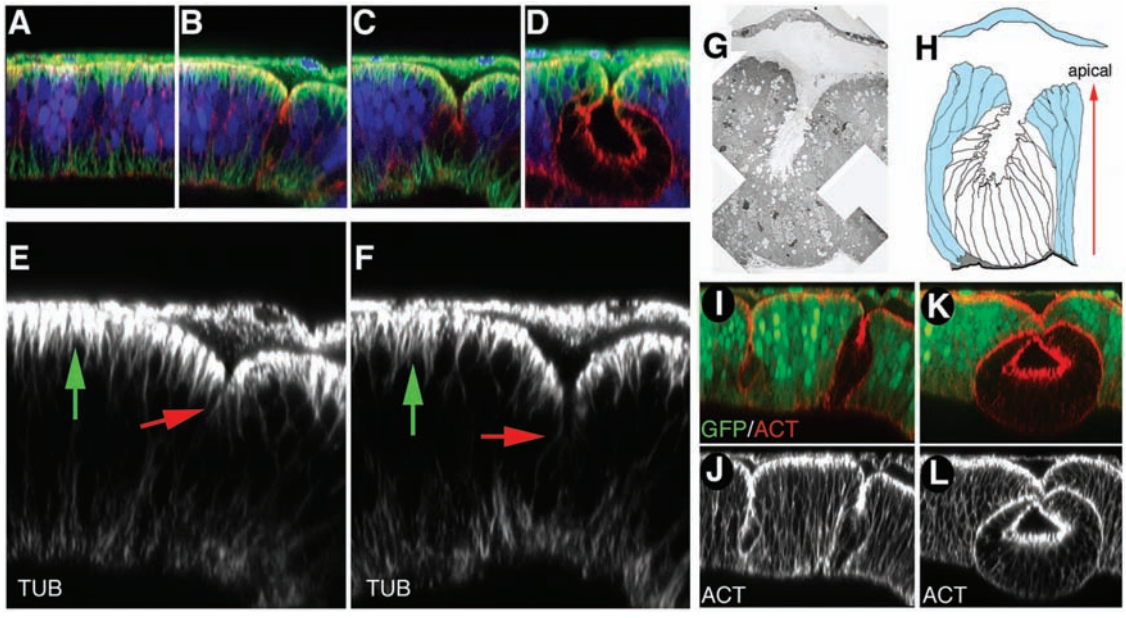

Fig. 4. Defective morphogenesis in extruding clones. (**A** to **D**) *tkv*^{xtr} clones lacking GFP (blue) and stained for F-actin (ACT, red), and microtubules (TUB, green). (A) In the absence of mutant clones, pseudostratified wing columnar cells feature a highly regular apical surface; the overlap between ACT and TUB staining appears as a yellow band. (B to D) Extruding *tkv*^{xtr} clones lose apical TUB, exposing red apical ACT. (**E** and **F**) Single-channel TUB staining from (B) and (C), respectively. Mutant cells (red arrows) autonomously lose the apical microtubule arrays present in neighboring control cells (green arrows). (**G**) Transmission electron microscopy sections confirm aberrant *tkv*^{xtr} cell shape. (**H**) Interpretive tracing of (G). (**I** to **L**) *tkv*^{4} clones show reduced basolateral cortical F-actin within the clone interior and ectopic F-actin accumulation at clone/nonclone boundaries.

DPP forms a medial-to-lateral gradient of signaling activity that antagonizes expression of the transcription factor encoded by *brinker* (*brk*) (Fig. 3A) (*26*). We made use of *brk-Gal4>UAS-srcEGFP* to mark the range of DPP/BMP signal and then examined cytoskeletal organization relative to the level of morphogen (Fig. 3, B to F). In confocal XZ sections through the wing disc, a gradation of columnar epithelial cell shape along the medial-lateral axis was immediately apparent, and this gradient of cell shape was further reflected in cytoskeletal organization. Although levels of F-actin localized to apical junctional complexes were fairly consistent across the disc, basolateral cortical F-actin levels were moderately reduced in lateral cells where DPP/BMP activity is low (Fig. 3C). Even more apparent, apical microtubule arrays were robust in medial cells where DPP/BMP is high, but tapered off to complete absence in the lateral *brk*-expressing domains (Fig. 3, D and E). Importantly, the density of basal microtubule arrays did not vary along the same axis, indicating that an apical-specific gradient of microtubule organization closely parallels the DPP/BMP morphogen gradient (Fig. 3E).

To test whether apical microtubule arrays, basolateral cortical F-actin, and epithelial cell shape were dependent on DPP/BMP signaling activity, we analyzed *T155>flp*-induced clones in greater detail (Fig. 4). Notably, the apical microtubule arrays were cell-autonomously eliminated in *tkv* mutant clones, even as basal microtubule networks were unperturbed (Fig. 4, B to F). Both large (early-induced) and small (late-induced) clones exhibited this phenotype, establishing the disruption of apical microtubule organization as an early and specific consequence of defective DPP/BMP signaling. Mutant cells also featured a subtle yet consistent reduction of F-actin at the basolateral cortex of cells on the clone interior, transient ectopic accumulation of F-actin at the apical adherens junctions, and ectopic accumulation of F-actin at boundaries between mutant cells and their wild-type neighbors (Fig. 4, I to L). Ultrastructurally, these phenotypes correlated with a clone-autonomous transition from pseudostratification to a simple columnar epithelial modality (Fig. 4, G and H). We conclude that the DPP/BMP morphogen gradient both correlates with and is required for a parallel gradient of epithelial organization in the developing wing columnar epithelium.

The data summarized here provide an initial conceptual link between DPP/BMP-dependent wing patterning and the spatial regulation of epithelial morphogenesis. A logical next step will be to connect transcriptional targets of the DPP/BMP pathway to candidate effectors of morphogenesis, particularly molecules that could influence the integrity of the apical microtuble cytoskeleton or cortical F-actin meshwork. Although our results could support a direct cytoskeletal function for DPP/BMP in the wing disc [perhaps similar to its proposed role in dorsal closure and thorax closure (*14*, *15*)], it is equally possible that DPP/BMP signaling drives epithelial morphogenesis by modulating cell adhesion. In this sense, the cell-autonomous disruption of apical microtubule arrays in *tkv* clones may be a result of abnormal apical cell-cell or cell-matrix adhesion. Consistent with this possibility, clonal loss of a chromosomal interval covering the DPP target *spalt* causes aberrant expression of the leucine-rich repeat cell-adhesion proteins *capricious* and *tartan* and segregation of mutant cells away from the epithelium (*20*). Furthermore, we found that hyperactivated DPP signaling caused defective epithelial organization in lateral wing disc cells but was not alone sufficient to induce apical microtubule arrays (*4*). Clearly, the ability to distinguish adhesive versus cytoskeletal roles for DPP/BMP will require further study of downstream effectors during multiple developmental processes.

The extrusion of *tkv* clones from *Drosophila* epithelia presents an interesting parallel to juvenile polyposis, a human genetic disorder characterized by the formation of gastrointestinal polyps and cancer (*27*–*30*). Not only does the formation of extruded epithelial polyps bear some superficial similarity to the phenotypes described here, but heritable juvenile polyposis has been linked to mutations in two loci: a type I BMP receptor (*27*) and the SMAD4 signal transducer (*28*). In this regard, the present study not only demonstrates a morphogenetic function for DPP/BMP in the *Drosophila* wing but may also indicate a broadly conserved role for DPP/BMP signaling in the patterned morphogenesis of developing and adult epithelia.

References and Notes

1. S. M. Cohen, in *The Development of Drosophila melanogaster*, M. Bate, A. Martinez Arias, Eds. (Cold Spring Harbor Laboratory, Cold Spring Harbor, NY, 1993), vol. 2, pp. 747–841.
2. C. Auerbach, *Trans. R. Soc. Edinb.* **58**, 787 (1936).
3. J. B. Duffy, D. A. Harrison, N. Perrimon, *Development* **125**, 2263 (1998).
4. M. C. Gibson, N. Perrimon, data not shown.
5. The FlyBase Consortium, *Nucleic Acids Res.* **31**, 172 (2003).
6. A. Penton *et al.*, *Cell* **78**, 239 (1994).
7. D. Nellen, M. Affolter, K. Basler, *Cell* **78**, 225 (1994).

8. T. J. Brummel *et al.*, *Cell* **78**, 251 (1994).
9. E. Ruberte, T. Marty, D. Nellen, M. Affolter, K. Basler, *Cell* **80**, 889 (1995).
10. D. Nellen, R. Burke, G. Struhl, K. Basler, *Cell* **85**, 357 (1996).
11. T. Lecuit *et al.*, *Nature* **381**, 387 (1996).
12. R. Burke, K. Basler, *Development* **122**, 2261 (1996).
13. M. A. Singer, A. Penton, V. Twombly, F. M. Hoffmann, W. M. Gelbart, *Development* **124**, 79 (1997).
14. E. Martin-Blanco, J. C. Pastor-Pareja, A. Garcia-Bellido, *Proc. Natl. Acad. Sci. U.S.A.* **97**, 7888 (2000).
15. M. G. Ricos, N. Harden, K. P. Sem, L. Lim, W. Chia, *J. Cell Sci.* **112**, 1225 (1999).
16. M. Affolter, D. Nellen, U. Nussbaumer, K. Basler, *Development* **120**, 3105 (1994).
17. E. Moreno, K. Basler, G. Morata, *Nature* **416**, 755 (2002).
18. T. Adachi-Yamada, K. Fujimura-Kamada, Y. Nishida, K. Matsumoto, *Nature* **400**, 166 (1999).
19. T. Adachi-Yamada, M. B. O'Connor, *Dev. Biol.* **251**, 74 (2002).
20. M. Milan, L. Perez, S. M. Cohen, *Dev. Cell* **2**, 797 (2002).
21. J. Rosenblatt, M. C. Raff, L. P. Cramer, *Curr. Biol.* **11**, 1847 (2001).
22. T. Adachi-Yamada, M. B. O'Connor, *J. Biochem.* (*Tokyo*) **136**, 13 (2004).
23. A. J. Ingram, L. James, H. Ly, K. Thai, J. W. Scholey, *Kidney Int.* **58**, 1431 (2000).
24. M. J. Galko, M. A. Krasnow, *PLoS Biol.* **2**, E239 (2004).
25. M. Ramet, R. Lanot, D. Zachary, P. Manfruelli, *Dev. Biol.* **241**, 145 (2002).
26. G. Campbell, A. Tomlinson, *Cell* **96**, 553 (1999).
27. J. R. Howe *et al.*, *Nat. Genet.* **28**, 184 (2001).
28. J. R. Howe *et al.*, *Science* **280**, 1086 (1998).
29. A. P. Haramis *et al.*, *Science* **303**, 1684 (2004).
30. M. G. Sayed *et al.*, *Ann. Surg. Oncol.* **9**, 901 (2002).
31. We thank E. Benecchi for assistance with transmission electron microscopy; M. Schober and J. David Lambert for critical readings of the manuscript; K. Gibson, S. Cherry, and C. Micchelli for helpful discussions; and G. Campbell, T. Kornberg, L. Raftery, K. Basler, R. Padgett, and the Bloomington Drosophila Stock Center for fly stocks. Our sincere apologies to colleagues whose work we were unable to cite owing to space constraints. N.P. is an Investigator of the Howard Hughes Medical Institute and M.C.G. is supported by the Jane Coffin Childs Memorial Fund for Cancer Research.

Supporting Online Material
www.sciencemag.org/cgi/content/full/307/5716/1785/DC1
Materials and Methods
Figs. S1 to S4
References and Notes

1 September 2004; accepted 11 January 2005
10.1126/science.1104751

Extrusion of Cells with Inappropriate Dpp Signaling from *Drosophila* Wing Disc Epithelia

Jie Shen and Christian Dahmann*

Decapentaplegic (Dpp) is a signaling molecule that controls growth and patterning of the developing *Drosophila* wing. Mutant cells lacking Dpp signal transduction have been shown to activate c-Jun amino-terminal kinase (JNK)–dependent apoptosis and to be lost from the wing disc epithelium. These observations have led to the hypothesis that Dpp promotes cell survival by preventing apoptosis. Here, we show that in the absence of JNK-dependent apoptosis, mutant cells lacking Dpp signal transduction can survive; however, they are still lost from the wing disc epithelium. This loss correlates with extensive cytoskeletal changes followed by basal epithelial extrusion. We propose that Dpp promotes cell survival within disc epithelia by affecting cytoskeletal organization.

Signaling by members of the transforming growth factor–β (TGF-β) protein family is critical for epithelial growth and differentiation, and inappropriate signaling is common in cancer (*1*, *2*). Dpp, a TGF-β superfamily member related to bone morphogenetic protein (BMP) 2/4, is required for growth and patterning of the wing primordium (wing disc pouch) in *Drosophila* (*3*). Inappropriately reduced Dpp signaling leads to smaller wing size, activation of the JNK pathway, and apoptosis (*4*, *5*). These and other observations have led to the hypothesis that Dpp acts as a survival factor for wing disc cells by preventing activation of the JNK-dependent apoptotic pathway (*5*–*8*).

To test this hypothesis, we analyzed the ability of cells mutant for the *Drosophila* gene *thickveins* (*tkv*), which encodes a receptor essential for Dpp signal transduction (*3*), and the gene *basket* (*bsk*), which encodes JNK (*9*), to survive within the developing wing disc pouch. Marked "twinspots" composed of sibling double-mutant *tkv bsk* clones of cells and wild-type clones of cells were generated within the same wing disc by Flp-mediated mitotic recombination (*10*). The ratio of *tkv*$^-$ *bsk*$^-$ clones to sibling wild-type clones was determined and is referred to as the frequency of *tkv*$^-$ *bsk*$^-$ clone recovery. When clones were induced in first instar larvae, the frequency of *tkv*$^-$ *bsk*$^-$ clone recovery in the wing disc pouch of late-third instar larvae was only 24% (n = 187), consistent with previous observations (*6*). Apoptosis was blocked in the mutant clones (fig. S1). *bsk*$^-$ clones were recovered at high frequency (97%, n = 100). The low frequency of *tkv*$^-$ *bsk*$^-$ clone recovery suggests that the loss of cells lacking Dpp signal transduction from the wing disc pouch is largely independent of JNK-mediated apoptosis (supporting online material text). Thus, Dpp must use additional mechanisms to prevent loss of cells from the wing disc pouch.

To elucidate these mechanisms, we generated *tkv*$^-$ *bsk*$^-$ clones in first instar larvae and analyzed their morphology in the wing disc pouch of late-third instar larvae. In the pseudostratified epithelium (Fig. 1A), *bsk*$^-$ clones displayed a normal shape (Fig. 1B). In contrast, *tkv*$^-$ *bsk*$^-$ clones were shorter along their apical-basal axis, had lost contact to the apical epithelial surface (Fig. 1C), and formed cyst-like structures with the apical cell membranes facing the center of the clone instead of the disc lumen (Fig. 1D). Furthermore, *tkv*$^-$ *bsk*$^-$ cells lost E-cadherin–based junctions to heterozygous neighboring cells and made E-cadherin–based junctions to other *tkv*$^-$ *bsk*$^-$ cells within the same clone (Fig. 1E). Clones mutant for both *mothers against dpp* (*mad*), which encodes a transcription factor essential for Dpp signal transduction (*3*), and *bsk* formed cyst-like structures similar to *tkv*$^-$ *bsk*$^-$ clones (fig. S2).

Epithelial cell shape is largely determined by the cytoskeleton. Cell shape changes leading to the formation of cyst-like structures could thus be due to cytoskeletal organization defects in *tkv*$^-$ *bsk*$^-$ cells. F-actin was enriched at the center of *tkv*$^-$ *bsk*$^-$ clones (Fig. 1F), whereas a dense apical network of microtubules, present in wild-type cells (*11*), was markedly reduced (Fig. 1, G and H). Basal microtubules appeared normal in *tkv*$^-$ *bsk*$^-$ cells (Fig. 1G). Both actin and microtubule cytoskeletons were normal in *bsk*$^-$ clones (Fig. 1B) (*12*). These data indicate that Dpp signaling is required to maintain normal cytoskeletal organization in wing disc pouch cells. Furthermore, the presence of an apical microtubule network correlated with Dpp signaling activity along the anterior-posterior axis of wild-type wing discs (fig. S3), suggesting that Dpp signaling also plays a role in determining position-specific aspects of the microtubule cytoskeleton.

To test whether the loss of *tkv*$^-$ *bsk*$^-$ clones was through the formation of the cyst-like structures, we generated *tkv*$^-$ *bsk*$^-$ clones at different times during development and determined the number of cyst-like structures and the frequency of *tkv*$^-$ *bsk*$^-$ clone recovery in late-third instar larvae (Fig. 2A). Twenty-four hours after clone induction, 99% of *tkv*$^-$ *bsk*$^-$ clones were recovered (n = 93) (Fig. 2B). Cells within clones still had contact to the apical epithelial surface, appeared to make normal E-cadherin–based junctions with

Max Planck Institute of Molecular Cell Biology and Genetics, Pfotenhauerstrasse 108, 01307 Dresden, Germany.

*To whom correspondence should be addressed. E-mail: dahmann@mpi-cbg.de